Available online at www.sciencedirect.com
ScienceDirect
JOURNAL OF RARE EARTHS, Vol. 32, No. 9, Sep. 2014, P. 806
JOURNAL OF RARE EARTHS
www.re-journal.com/en/

Combustion synthesis, characterization and luminescence properties of barium aluminate phosphor

A.H. Wako[1,*], F.B Dejene[1], H.C Swart[2]

(1. Department of Physics, University of the Free State (Qwaqwa Campus), Private Bag X13, Phuthaditjhaba 9866, South Africa; 2. Department of Physics, University of the Free State, P.O. Box 339, Bloemfontein 9300, South Africa)

Received 25 September 2013; revised 24 April 2014

Abstract: The blue-green emitting Eu^{2+} and Nd^{3+} doped polycrystalline barium aluminate ($BaAl_2O_4:Eu^{2+},Nd^{3+}$) phosphor, was prepared by a solution-combustion method at 500 ºC without a post-annealing process. The characteristic variation in the structural and luminescence properties of the as-prepared samples was evaluated with regards to a change in the Ba/Al molar ratio from 0.1:1 to 1.4:1. The morphologies and the phase structures of the products were characterized by scanning electron microscopy (SEM), transmission electron microscopy (TEM), X-ray diffraction (XRD) and X-ray photoelectron spectroscopy (XPS), while the optical properties were investigated using ultra-violet (UV) and photoluminescence (PL) spectroscopy, respectively. The XRD and TEM results revealed that the average crystallite size of the $BaAl_2O_4:Eu^{2+},Nd^{3+}$ phosphor was about 70 nm. The broad-band UV-excited luminescence of the phosphors was observed at λ_{max}=500 nm due to transitions from the $4f^65d^1$ to the $4f^7$ configuration of the Eu^{2+} ion. The PL results indicated that the main peaks in the emission and excitation spectrum of phosphor particles slightly shifted to the short wavelength due to the changes in the crystal field due to the structure changes caused by the variation in the quantity of the Ba ions in the host lattice.

Keywords: $BaAl_2O_4:Eu^{2+},Nd^{3+}$; persistence luminescence; Eu^{2+} and Nd^{3+} doping; rare earths

Rare earth doped aluminates form a group of luminescence materials which exhibit high stability, brightness, and versatile industrial processing characteristics suitable for manufacture of lighting and display devices[1,2]. They exhibit high quantum efficiency in the visible region[3]. The Eu^{2+} doped solid state materials usually show strong broad band luminescence with a short decay time of the order of some tens of nanoseconds[4]. The very short decay time and strong intensity of the luminescence arise from the allowed states of the electronic transitions both in the excitation and emission. The luminescence is very strongly affected by changes in the structure of the host and can range from the ultraviolet to the red region of the electromagnetic spectrum. The high intensity emission of Eu^{2+} finds important industrial applications in, for example, the tricolour low pressure mercury fluorescence lamps. The discovery of the plasma display panel (PDP) and light-emitting diode (LED) has contributed significantly to comprehensive studies for large-scale flat panel display and lighting devices[5]. Plasma display panels (PDPs), are gaining considerable popularity because of its obvious merits, such as a fast response, a wide viewing angle, large screen, low energy consumption and high scalability[6].

Eu^{2+} and Nd^{3+}-doped alkaline earth aluminate phosphors exhibit afterglow which is visible to the naked eye for longer duration after exposure to a fluorescent light or sunlight. The synthesis of oxide phosphors has been achieved by a variety of methods. The solution-combustion process is very simple, safe, energy saving and takes only a few minutes. The technique makes use of the heat energy from the redox exothermic reaction at a relatively low igniting temperature between metal nitrates and urea as fuel. In the present work, $BaAl_2O_4:Eu^{2+},Nd^{3+}$ materials were prepared with different Ba/Al molar ratios and constant Eu^{2+} and Nd^{3+} concentrations. The effects of this on the stability, homogeneity and structure as well as persistence luminescence were presented and discussed based on the analyses of the X-ray diffraction (XRD), X-ray photoelectron spectroscopy (XPS), scanning electron microscopy (SEM) and transmission electron microscopy (TEM) imaging as well as photoluminescence spectroscopy (PL) studies.

1 Experimental

1.1 Synthesis

$BaAl_2O_4:Eu^{2+},Nd^{3+}$ phosphors were synthesized using the solution-combustion method under atmospheric pressure without any post treatment. The starting raw materials used in the experiment included various proportions of analytical pure grade $Ba(NO_3)_2$, $Al(NO_3)_3·9H_2O$, $Eu(NO_3)_3·5H_2O$, $Nd(NO_3)_3$, and urea

Foundation item: Project supported by South African National Research Foundation (NRF)

* **Corresponding author:** A.H. Wako (**E-mail:** wakoah@qwa.ufs.ac.za; **Tel.:** +27-51-4012926)

DOI: 10.1016/S1002-0721(14)60145-9

$(CO(NH_2)_2)$. No flux was added. The precursors were prepared with different Ba/Al molar ratios of 0.1:1, 0.4:1, 0.7:1 and 1.4:1, respectively. The doping concentrations of both Eu^{2+} and Nd^{3+} were kept constant at 0.2 mol.%. A minimum amount of distilled water together with excess amount of urea was added and then thoroughly mixed at room temperature using a magnetic stirrer for 15 min without heating to obtain uniform aqueous solutions. The solutions were introduced into a muffle furnace previously maintained at 500 °C. Dehydration occurred as the solution boiled and decomposed letting off large amounts of gases (CO_2, NO_2 and NH_4). The mixture then frothed and swelled enormously into foam. Spontaneous ignition and smouldering occurred which gradually led to an explosion rupturing the foam with a flame that glows to incandescence producing white foamy and voluminous $BaAl_2O_4:Eu^{2+},Nd^{3+}$. The foam was taken out of the muffle furnace, cooled then milled resulting in a dry, usually crystalline, fine white oxide powders of $BaAl_2O_4:Eu^{2+},Nd^{3+}$. The whole combustion process took about 5 min. The powders were stored in glass sample bottles for characterization.

1.2 Characterization

The structure and phase purity of the phosphor samples was checked with a Bruker-AXS D8 Advance X-ray diffractometer (Bruker Corporation of Germany) operating at 40 kV and 4 mA using Cu Kα=0.15406 nm. The morphologies of the phosphor powders were obtained by using a Shimadzu Superscan SSX-550 SEM coupled with an energy dispersive X-ray spectrometer (EDS) for elemental composition. For analysis of molecular bonding, binding energy, chemical and valence state of the samples, XPS was done using a PHI 5000 Versa probe — scanning XPS microprobe. Absorption spectra were recorded using a Perkin Elmer Scan-Lambda 950 UV-Vis spectrophotometer. The PL excitation and emission spectra were measured at room temperature using a Cary Eclipse luminescence spectrometer (model LS-55) with a built-in 150 W xenon flash lamp as the excitation source and a grating to select a suitable excitation wavelength.

2 Results and discussion

2.1 XRD analysis

Fig. 1 shows the XRD pattern of different phases of $BaAl_2O_4$ along with the (hkl) values for the various peaks recorded from the $BaAl_2O_4:Eu^{2+},Nd^{3+}$ samples with varying Ba/Al concentrations. Non-stoichiometric Ba/Al molar ratio were selected in order to investigate how the different phases formed by a shortage or excess of Ba ions as compared to Al ions would affect the luminescence properties of the phosphors. The results of X-ray phase analysis of the as-prepared powders at 500 ºC revealed that several crystalline phases are formed depending on the ratio of these main components of the host[7]. The patterns could separately be indexed to the various hexagonal systems of the $BaAl_2O_4$ and the lattice parameters were in agreement with the JCPDS data 072-0387 and 075-0707. It is observed that the peaks for hexagonal $BaAl_2O_4$ with space group $P6_322$ began to appear distinctly producing the highest intensity for samples with Ba/Al molar ratio of 0.7:1. Impurity phases including Eu_2O_3, Ba_3Al_5, and Ba_7Al_{10} could be identified. These impurities are attributed to the unreacted reagents that could be present in the as-prepared phosphor. Line broadening features are characteristics of samples exhibiting smaller particle size, indicating that the phosphor nanocrystallines can be prepared in a far low temperature (about 500 °C). It is well known that broadening occurs in the diffraction rings as the particle size of the powders

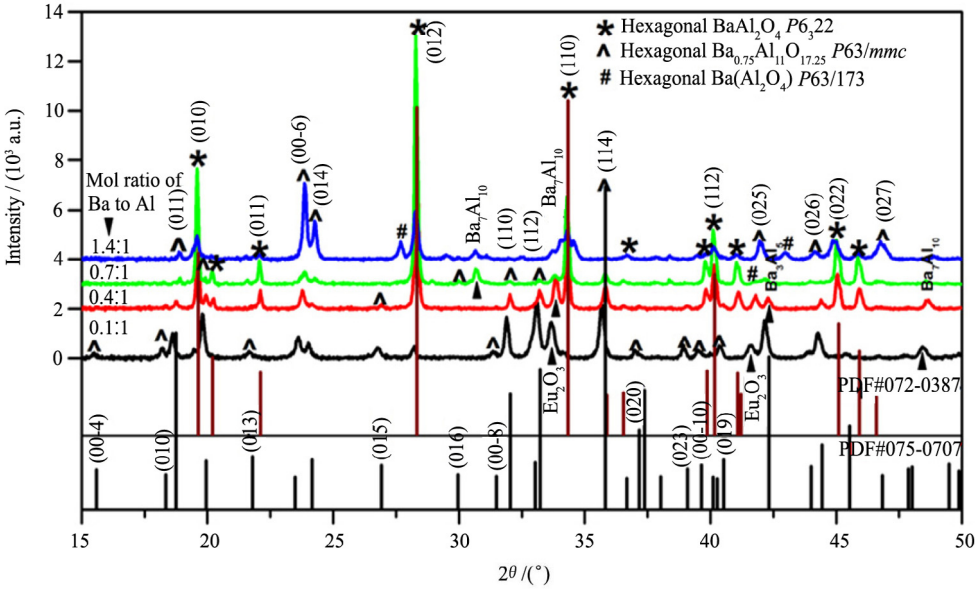

Fig. 1 Effect of varying Ba:Al molar ratios on the XRD structure of the $BaAl_2O_4:Eu^{2+},Nd^{3+}$ phosphor as compared with JCPDS #72-0387 and 075-0707 of hexagonal $BaAl_2O_4$

decreases. The average crystallite size deduced according to the Scherrer's equation using full-width at the half-maximum (FWHM) data[8] was 70 nm.

The crystal structure of $BaAl_2O_4$ is depicted in Fig. 2(a) and (b). It belongs to the $P6_322$ space group and has a stuff tridymite (hexagonal) structure with lattice parameters a=0.5218 nm and c=0.8781 nm[9]. Usually it consists of two types of tetrahedral rings: trigonal and asymmetrical rings. The trigonal rings, comprising a quarter of the total number of rings, contain in their centre the Ba atoms. In the asymmetrical rings the Ba atoms are located at the general position (6c) site (Fig. 2(b)).

2.2 XPS analysis

Fig. 3(a), (b) and (c) shows the fitted XPS spectra of $BaAl_2O_4$:Eu^{2+},Nd^{3+} phosphor powder with a Ba:Al molar ratio of 0.1:1. From Fig. 3(a) it can be seen that the 3d spectrum for Ba has two peaks of O–Ba–O bonds for the $3d_{5/2}$ as well as the $3d_{3/2}$ existing within the $BaAl_2O_4$:Eu^{2+},Nd^{3+} structure at 779.2, 780.8 and 794.6, 796.1 eV, respectively. These two peaks can be attributed to have emanated from the two Ba^{2+} sites of $BaAl_2O_4$. A single peak depicted in Fig. 3(b) presents the Al 2p spectrum with a typical Ba–Al–O bond at 74.3 eV. This could be characteristic of all species in the AlO_4 tetrahedra[10] Fig. 3(c) shows two fitted peaks of the 1s spectrum for O at 530.2 and 531.7 eV respectively which arise from the Ba–Al–O bonds within the $BaAl_2O_4$ matrix. The binding energy (E_b) of O 1s in $BaAl_2O_4$ has been reported to be at 531.3 and 529.6 eV[10]. The E_b=

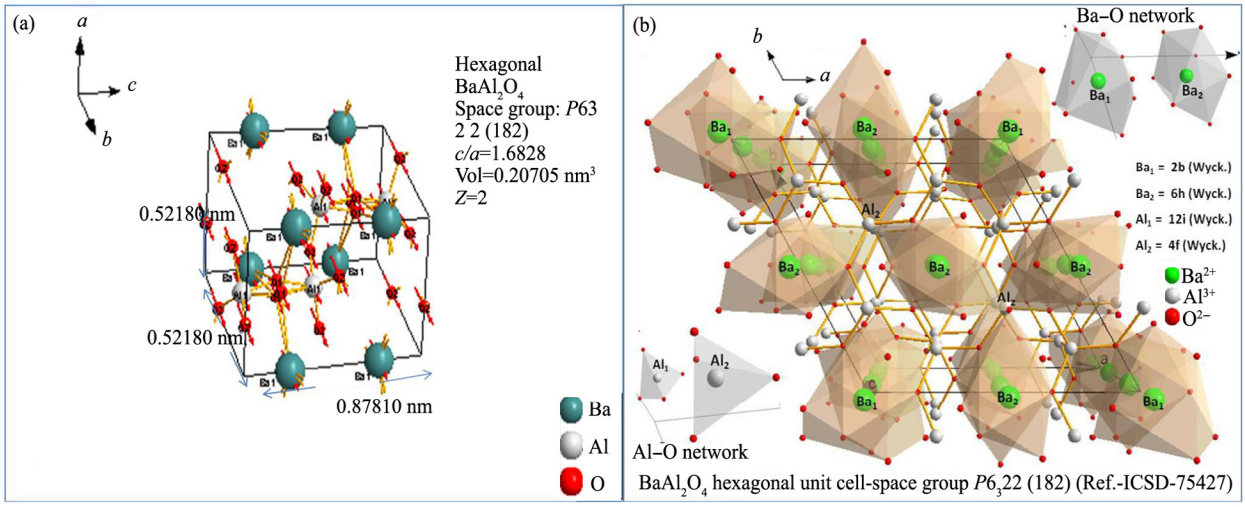

Fig. 2 The hexagonal crystal structure of $BaAl_2O_4$ viewed along the (111) direction

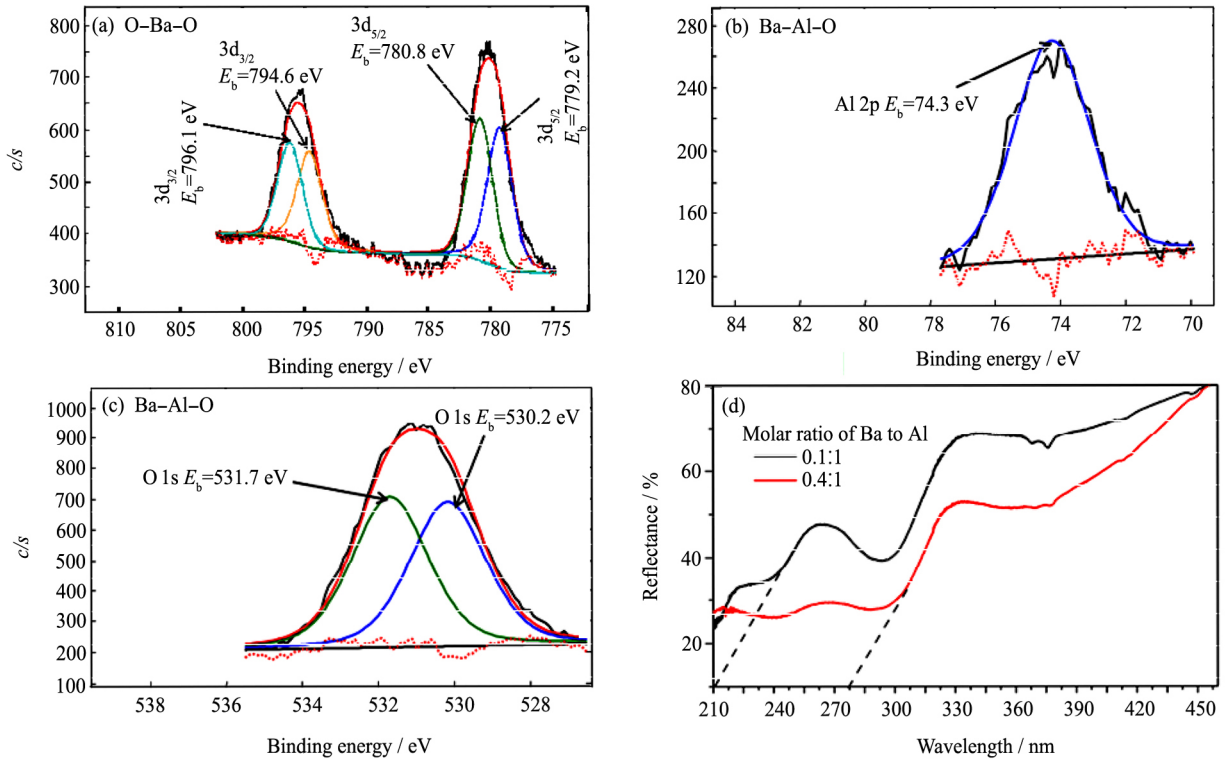

Fig. 3 Fitted XPS graphs of $BaAl_2O_4$:Eu^{2+},Nd^{3+} sample with Ba/Al molar ratio of 0.1:1 (a)-(c) and UV reflectance spectra for Ba/Al molar ratio of 0.1:1 and 0.4:1, respectively (d)

531.3 eV could be ascribed to the characteristics of O species in the surface hydroxyl (OH) groups from H_2O molecules absorbed by the $BaAl_2O_4$ material[11] as well.

The optical property of a material revealed by its UV-reflectance/absorption spectrum tells about the energy separation between the filled valence band and the empty conduction band i.e. the band gap. Optical excitation of electron across the band gap is strongly allowed, producing an abrupt increase in absorption at the wavelength corresponding to the band gap energy. This feature in the optical spectrum is known as the optical absorption edge[12]. Fig. 3(d) presents the diffuse reflectance spectra of $BaAl_2O_4$:Eu^{2+},Nd^{3+} samples with Ba/Al molar ratio of 0.1:1 and 0.4:1. It reveals that reflectance decreases with an increase in the Ba:Al molar ratio. The band gaps (E_g) corresponding to the absorption edges of λ=210 nm and λ=280 nm are found to be 5.9 and 4.43 eV for samples with Ba/Al molar ratio of 0.1:1 and 0.4:1, respectively, which further reveals that as the Ba:Al molar ratio increased the band gap decreased. Such changes in the host matrix leading to the shift of the band gap width also caused changes in the energy of the Eu^{2+} ion in the transition process[13].

2.3 SEM, TEM and EDS analysis

Fig. 4 shows the micrographs of the as-prepared $BaAl_2O_4$:Eu^{2+},Nd^{3+} material. Figs. 4 (a) and (b) are the representative SEM micrographs taken for Ba/Al molar ratio of 0.4:1 and 0.7:1, respectively. The nanostructures crystallized to form fine, regular hexagonal platelets exhibiting smooth surface and well-developed faces with size around 70 nm calculated from the Scherrer method. The endothermic reactions during the solution-combustion process are characterised by decomposition and removal of nitric oxides and significantly vary depending on the precursor ingredients and the ratio of metal nitrate to urea[14]. Consequently, the surfaces of the samples reveal pores and voids, which may be attributed to these evolved gases during combustion. The presence of hexagonal platelets with well-developed faces seem to dominate the morphology of the samples with Ba/Al molar ratio of 0.7:1 (Fig. 4(b)). Phosphors with regular morphology are well known to improve the packing density, slurry properties and improve the luminescence of phosphor[15]. This explains the high luminescence intensity obtained by the sample with Ba/Al molar ratio of 0.7:1 in the next section.

Fig. 4(c) presents the TEM image taken for Ba/Al molar ratio of 0.1:1. It can be seen that the $BaAl_2O_4$:Eu^{2+},Nd^{3+} nanocrystals exhibit an ideal spherical morphology which is more beneficial at increasing packing densities and brightness than irregularly shaped particles[16]. Furthermore, it reveals that the synthesized grain sizes calculated using Scherrer's formula are in the same range of 45–74 nm of the TEM results. The EDS spectrum of Fig. 4(d) confirms the elemental composition of the phosphors. However the very low concentration of the rare earth dopants was the reason for their tiny peaks in the EDS spectra.

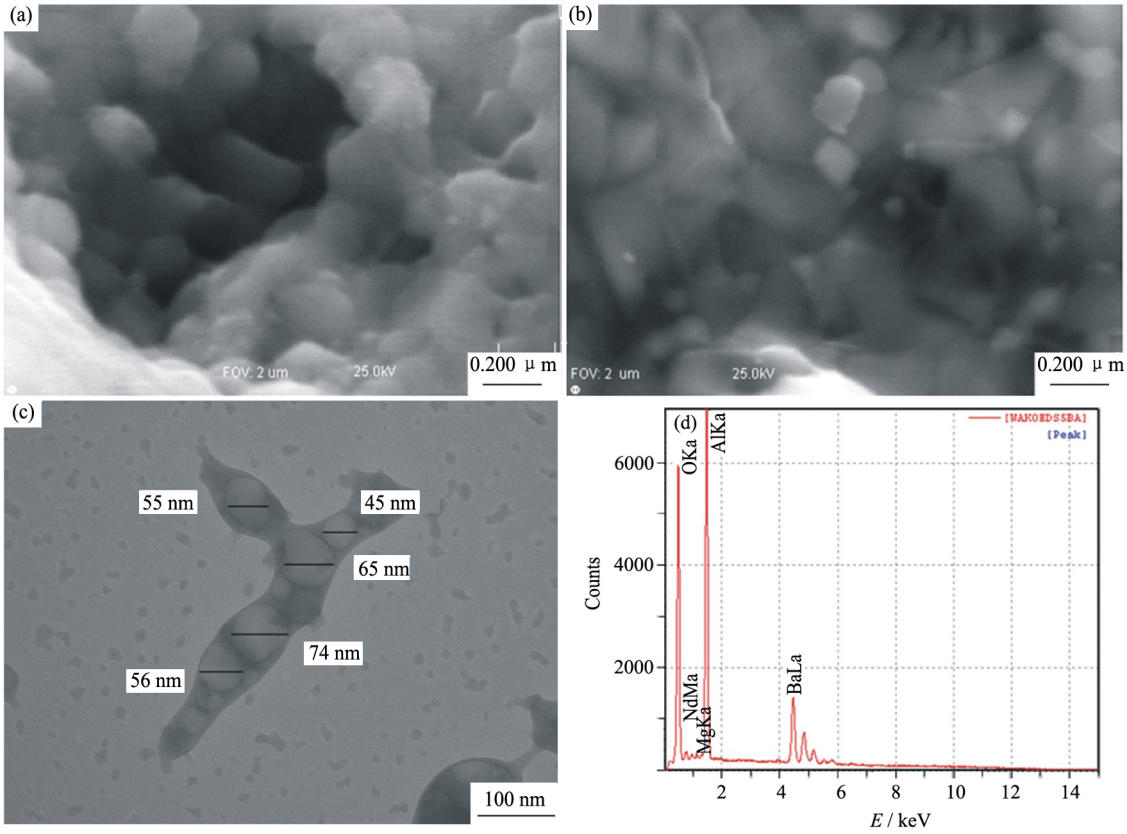

Fig. 4 SEM images of samples with Ba/Al molar ratios of 0.4:1 and 0.7:1 at 2 μm FOV (a) and (b), TEM micrograph for the 0.1:1 Ba/Al molar ratio on a 100 nm scale bar (c) and the EDS spectra of the $BaAl_2O_4$:Eu^{2+}, Nd^{3+} phosphor (d)

2.4 PL analysis

Fig. 5 shows the effect of varying the Ba:Al molar ratios on the luminescence characteristics of the $BaAl_2O_4$:Eu^{2+},Nd^{3+} phosphor. From Fig. 5(a) there is an excitation peak at around 333 nm in the excitation spectrum (λ_{em}= 500 nm) which is in conformity with the absorption of the host $BaAl_2O_4$ as observed in the absorption results earlier in this study. Two maxima curve fits, peaking at 490 and 525 nm, were observed in the luminescence spectra of $BaAl_2O_4$:Eu^{2+},Nd^{3+} (Fig. 5(c)) which arise from the two emissions of Eu^{2+} in the two Ba^{2+} sites within in the $BaAl_2O_4$ structure. These are due to the transitions from the lowest ^2D level of the excited $4f^65d^1$ configuration to the ground $^8S_{7/2}$ level of the $4f^7$ configuration of the Eu^{2+} ion[17].

The emission intensity at 490 nm was observed to be higher relative to the one at 525 nm (Fig. 5(c)) indicating that the Eu^{2+} ions preferred occupying one of the Ba^{2+} sites. Both Ba^{2+} sites are coordinated with nine oxygen (O) ions and the sites are similar in average size ($d(Ba–O)_{Ave}$=0.286 and 0.287 nm). However, the lower symmetry site also has shorter Ba–O distances (0.269 nm) corresponding to those typical of Eu^{2+}–O (0.268 nm)[18]. According to the crystal structure, the first Ba^{2+} site (2a) has the multiplicity of two and a site symmetry of C3 while the second one (6c) has six and C1. It would therefore seem reasonable that this 6c site is filled preferentially. This is also supported by the higher PL intensity as a result of contribution from six instead of two Eu^{2+} ions[17]. Slight shifts in peak positions can be observed in both the excitation and emission spectra (Fig. 5(a) and (b)) which may be ascribed to structure changes caused by the variation in the quantity of Ba ions in the host. The changes in the structure shifts the peak position of Eu^{2+} ions since the $4f^65d^1 \rightarrow 4f^7$ of Eu^{2+} is parity allowed transition in addition to the oscillation strength which is strongly affected by the crystal field due to the extended nature of the 5d wave function[19]. The narrow emissions in red region at 615 nm arise from the f-f transitions of the remnant unreduced Eu^{3+} ions.

From the decay curves of Fig. 5(d), the effect of the increase in number of Ba ions is very clear. It can be seen that the Ba/Al=0.7:1 gives higher luminescence intensity in agreement with both the excitation and emission spectra. The inset graph of Fig. 5(d) shows the natural log of intensity ln(I) vs time (t) plot giving a number of straight lines. The decay curves were fitted using the second order exponential decay equation[20]:

$$I = A_1 \exp\left(\frac{-t}{\tau_1}\right) + A_2 \exp\left(\frac{-t}{\tau_2}\right) \quad (1)$$

where I is the phosphorescence intensity, A_1 and A_2 are constants, t is the time after switching off the excitation source, and τ_1 and τ_2 are decay times for the exponential components representing the decay rate for the fast and

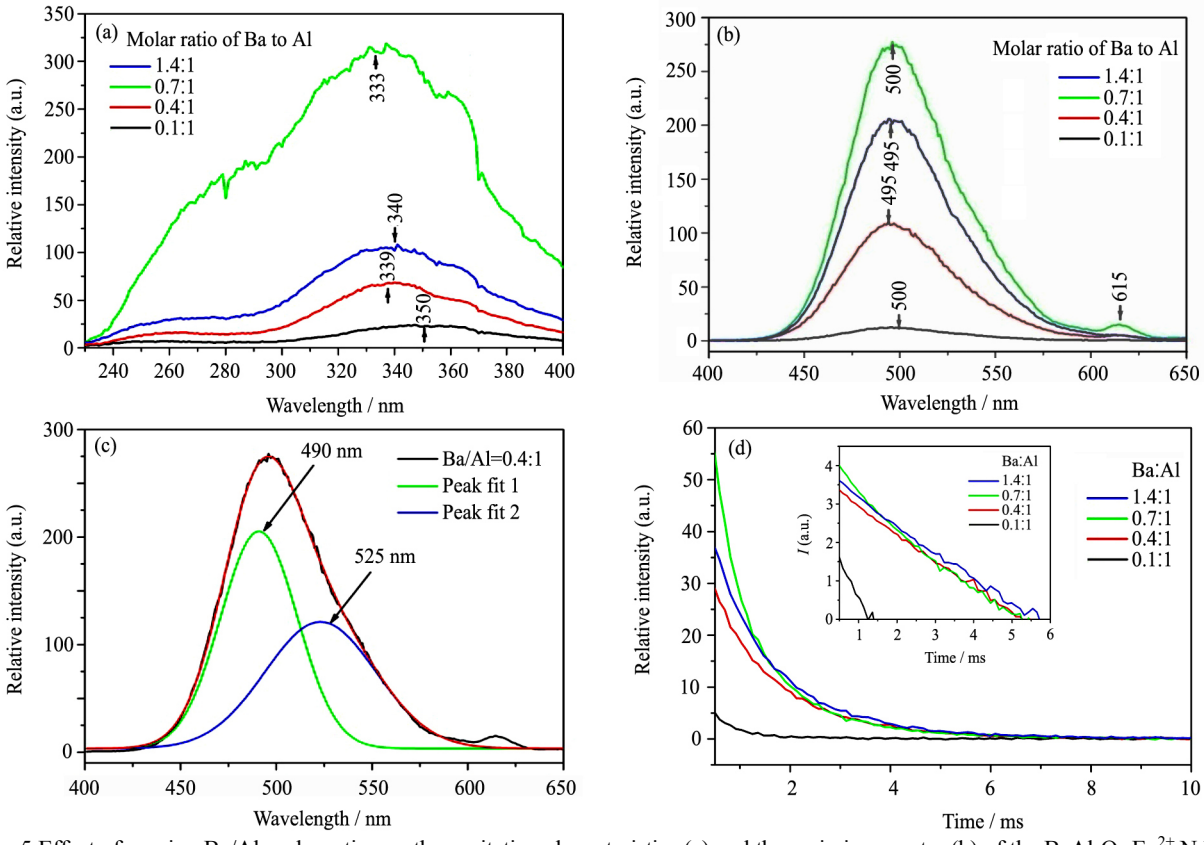

Fig. 5 Effect of varying Ba/Al molar ratios on the excitation characteristics (a) and the emission spectra (b) of the $BaAl_2O_4$:Eu^{2+},Nd^{3+} phosphor, two maxima curve fits peaking at 490 and 525 nm (c), and decay curves of the $BaAl_2O_4$:Eu^{2+},Nd^{3+} phosphor (d) (The inset graph shows the natural log of intensity ln (I) vs time (t) plot for the samples)

slow exponential decay components, respectively. The second order exponential decay fit may be attributed to a number of possibilities; (i) variations in the concentration of dopants which arise from their non-uniform distribution in the host matrix, (ii) the probability of non-radiative decays for lanthanide ions at or near the surface could be different from those at larger depths of the particles and (iii) energy transfer from donor to activators[21,22].

We consider parameters with the lowest and highest intensity shown in the inset of Fig. 5(d) since the parameters in between are too close to each other that accuracy of results could not be guaranteed. Table 1 shows decay times for the fitted curves of all the samples. It shows that the initial luminescence intensity and the decay time of phosphors are greatly affected with the increase in the Ba/Al molar ratios. The result of sample with Ba:Al molar ratio of 0.7:1 shows good agreement with the emission spectrum within the range of experimental errors. The long decay time and strong intensity of the luminescence is due to the allowed nature of the electronic inter configurational transitions both in the excitation and emission which makes this material suitable for plasma display panel PDP applications.

Table 1 Results for fitted decay curves of the phosphor powders with different Ba:Al molar ratios

Ba:Al molar ratio	0.1:1	0.4:1	0.7:1	1.4:1
Fast(τ_1)	0.84±0.15	1.54±0.02	0.46±0.008	0.73±0.04
Slow (τ_2)	2.8±0.05	0.55±0.04	1.42±0.02	1.61±0.03

3 Conclusions

Blue-green emitting $BaAl_2O_4:Eu^{2+},Nd^{3+}$ phosphor was synthesised by a solution-combustion method. The influences of the varying quantity of Ba on the structural and luminescent properties of the phosphor were studied. SEM results indicated that the nanostructures crystallized to form fine, regular hexagonal platelets exhibiting smooth surface and well-developed faces. XRD analysis revealed several crystalline phases formed depending on the ratio of the main components (Ba/Al) of the host. XPS results showed that the 3d spectrum for Ba had two peaks of O–Ba–O bonds for $^3d_{3/2}$ and $^3d_{5/2}$ existing within the $BaAl_2O_4:Eu^{2+},Nd^{3+}$. The absorption spectra showed the absorption edge at λ=210 nm and λ=280 nm for which the corresponding band gaps (E_g) were 5.9 and 4.43 eV respectively. The long decay time and strong luminescence intensity of $BaAl_2O_4:Eu^{2+},Nd^{3+}$ makes it suitable for PDP applications.

Acknowledgements: The authors are immensely grateful to the Prestige Cluster Bursary Program of the University of the Free State for financial support towards this project. The authors also thank the University of the Free State Physics Department for assistance with the research technique systems used to characterize materials for this study.

References:

[1] Justel T, Krupa J, Wiechert D. VUV spectroscopy of luminescent materials for plasma display panels and Xe discharge lamps. *J. Lumin.*, 2001, **93**: 179.

[2] Zhou L Y, Huang J L, Yi L H, Gong M L, Shi J X. Luminescent properties of $Ba_3Gd(BO_3)_3:Eu^{3+}$ phosphor for white LED applications. *J. Rare Earths*, 2009, **27**: 54.

[3] Palilla F C, Levine A K, Tomkus M R. Fluorescent properties of alkaline earth aluminates of the type MAl_2O_4 activated by divalent europium. *J. Electrochem. Soc.*, 1968, **115**: 642.

[4] Blasse G, Grabmaier B C. Luminescent Materials. Berlin: Springer Verlag, 1994. 232.

[5] Justel T, Nikol H. Optimization of luminescent materials for plasma display panels. *Adv. Mater.*, 2000, **12**: 527.

[6] Kim C H, Bae H S, Pyun C H, Hong G H. Phosphors for plasma display panels. *J. Korean Chem. Soc.*, 1998, **5**(42): 588.

[7] Kimura S, Bannai E, Shindo I. Phase relations relevant to hexagonal barium aluminates. *Mater. Res. Bull.*, 1982, **17**(2): 209.

[8] Cullity B D. Elements of X-ray Diffraction (2nd edn.), Reading, MA: Addison-Wesley, 1997. 102.

[9] Jia D, Wang X, Van der Kolk E, Yen W M. Site dependent thermoluminescence of long persistent phosphorescence of $BaAl_2O_4:Ce^{3+}$. *Opt. Commun.*, 2002, **204**: 247.

[10] Zhang L, Wang L, Zhu Y. Synthesis and performance of $BaAl_2O_4$ with a wide spectral range of optical absorption. *Adv. Func. Mater.*, 2007, **17**: 3781.

[11] Lephoto M A, Ntwaeaborwa O M, Swart H C, Botha J R, Mothudi B M. Synthesis and characterization of $BaAl_2O_4:Eu^{2+}$ co-doped with different rare earth ions. *Physica B*, 2012, **407**(10): 1603.

[12] Ziyauddin M, Brahme N, Bisen D P, Kher R S. Combustion synthesis and thermoluminescence studies of UV-irradiated $CaAl_2O_4$:Eu nanophosphor. *Lumin. Appl.*, 2013, **3**(1): 76.

[13] Ding Z, Yu Z N, Zhang D P, Xue W, Wang W Y. Research on fabricating technique of Ba-Al-S:Eu sputtering target. *J. Rare Earths*, 2009, **27**: 398.

[14] Sarkisov P D, Popovich N V, Zhelnin A G. Luminophores based on strontium aluminates produced by the sol-gel method. *Glass Ceram.*, 2003, **60**: 309.

[15] Teng X M, Zhang W D, Hu Y S, Zhao C L, He H Q, Huang X W. Effect of flux on the properties of $CaAl_2O_4:Eu^{2+}$, Nd^{3+} long afterglow phosphor. *J. Alloys Compd.*, 2008, **458**: 446.

[16] Jeon B S, Hong G Y, Yoo Y K, Yoo J S. And spherical $BaMgAl_{10}O_{17}:Eu^{2+}$ phosphor prepared by aerosol pyrolysis technique for PDP applications. *J. Electrochem. Soc.*, 2001, **148**: 128.

[17] Stefani R, Rodrigues L C V, Carvalho C A A, Felinto M C F, Brito H F, Lastusaari M, Hölsä J. Persistent luminescence of Eu^{2+} and Dy^{3+} doped barium aluminate ($BaAl_2O_4:Eu^{2+},Dy^{3+}$) materials. *Opt. Mater.*, 2009, **31**: 1815.

[18] Shannon R D. Crystal physics, diffraction, theoretical and general crystallography. *Acta Crystallogr.*, 1976, **A32**: 751.

[19] Zeng Q H, Tanno H, Egoshi K, Tanamachi N, Zhang S X. $Ba_5SiO_4Cl_6:Eu^{2+}$: An intense blue emission phosphor under vacuum ultraviolet and near-ultraviolet excitation. *Appl. Phys. Lett.*, 2006, **88**: 051906.

[20] Sakai R, Katsumata T, Komuro S, Morikawa T. Effect of composition on the phosphorescence from $BaAl_2O_4:Eu^{2+}$, Dy^{3+} crystals. *J. Lumin.*, 1999, **85**: 149.

[21] Stouwdam J W, van Veggel F C J M. Near-infrared emission of redispersible Er^{3+}, Nd^{3+}, and Ho^{3+} doped LaF_3 nanoparticles. *Nano Lett.*, 2002, **2**: 733.

[22] Singh N S, Ningthoujam R S, Yaiphaba N, Vasta R K, Singh S D. Lifetime and quantum yield studies of Dy^{3+} doped $GdVO_4$ nanoparticles: concentration and annealing effect. *Appl. Phys.*, 2009, **105**: 064303.